Effect of the Methyl Internal Rotation Barrier Height on CH−Stretching Overtone Spectra

Zimei Rong, Daryl L. Howard, and Henrik G. Kjaergaard*

Department of Chemistry, University of Otago, P.O. Box 56, Dunedin, New Zealand

Received: February 3, 2003; In Final Form: April 14, 2003

The coupling of CH stretching with methyl internal rotation (torsion) causes complexity in methyl CH stretching overtone spectra. We have used a CH stretching methyl torsion model to simulate the methyl band overtone profiles. Room-temperature vapor phase overtone spectra of acetic acid ($\Delta v_{CH} = 4-5$) and 2-methylfuran ($\Delta v_{CH} = 4-5$) have been recorded in the methyl CH stretching regions. These combined with previously studied molecules acetone, acetaldehyde, toluene, methylpyridines, and xylenes provide a series of molecules with gradually varying barrier heights.

Introduction

The bond length and frequency of a CH bond depend on its chemical environment.[1,2] The CH stretching frequency and anharmonicity in a methyl group are dependent on the torsional angle; thus, it is necessary to include torsion in the methyl Hamiltonian. Successful simulations of methyl CH stretching overtone spectra have been obtained for a few molecules with low torsional barriers with models in which the CH stretching vibration is described by a harmonically coupled anharmonic oscillator (HCAO) local mode model and the methyl torsion in a rigid rotor basis.[3−5] In the CH stretching torsional models, the potential energy, frequency, and anharmonicity are approximated by a Fourier series in the torsional angle, and the dipole moment function by a Fourier series in the torsional angle and a Taylor series in the CH stretching displacement coordinates.

In CH stretching overtone spectra, one usually observes one peak for each of the nonequivalent bonds.[6] If the barrier to torsion is large, then the methyl group is effectively fixed in one position on the time scale of the CH vibrations. In dimethyl ether, where the barrier height is 909 cm^{-1},[7] one observes two transitions corresponding to the in-plane CH bonds and the out-of-plane CH bonds.[8] These spectra have been successfully modeled by the HCAO local mode model without torsion.[8]

If the torsional barrier is very low (5 cm^{-1}, as in toluene), there is effectively free rotation of the methyl group, and a more complex spectrum is observed. In the $\Delta v_{CH} = 4$ overtone methyl region, this spectrum has three peaks.[1] The central peak was earlier assigned to the "freely rotating methyl group" band with the other bands assigned to the in plane and out of plane CH stretches.[1] As mentioned, the toluene methyl overtone spectrum has been simulated in our CH stretching torsion model.[5] However, as the barrier height approaches 100 cm^{-1}, changes from the low barrier "three peak spectrum" have recently been observed.[2]

The aim of the present paper is to study how the methyl band profile evolves with the barrier height. Of interest are barrier heights around 150−400 cm^{-1}. We have recorded vapor phase CH stretching overtone spectra in the $\Delta v_{CH} = 4$, 5 regions for acetic acid and 2-methylfuran and in the $\Delta v_{CH} = 4-6$ regions for acetaldehyde, molecules which have suitable barrier heights. The methyl band overtone spectra of acetaldehyde in the regions of $\Delta v_{CH} = 4-7$ have been recorded by Fang et al.[9] and in the region of $\Delta v_{CH} = 1-4$ by Hanazaki et al.;[10] however, the previous spectra have shown little detail in the methyl regions relevant for this study. We compare the methyl bands in these spectra with previously recorded spectra of acetone;[8] toluene;[11] *o*-, *m*-, and *p*-xylene;[12] and 2-, 3-, and 4-methylpyridine.[2] We suggest that the methyl CH stretching overtone spectrum could be an alternative way to estimate barrier heights complementary to microwave and IR techniques currently used.

Experimental Section

The samples of acetic acid (99.8%) and acetaldehyde (99.5%) from BDH Laboratory Supplies and 2-methylfuran (99%, Aldrich) were used without further purification except for degassing. The methyl overtone spectra of 2-methylfuran (19 Torr for $\Delta v_{CH} = 4$, 75 Torr for $\Delta v_{CH} = 5$), acetaldehyde (60 Torr) and acetic acid (9 Torr with 149 Torr Argon buffer gas) in the regions of $\Delta v_{CH} = 4$ and 5 were recorded using our intracavity titanium:sapphire laser photoacoustic spectrometer with the mid- and short-wave optics, respectively. An intracavity dye laser photoacoustic spectrometer was used to record the methyl overtone spectra of acetaldehyde (391 Torr, R6G dye) in the $\Delta v_{CH} = 6$ region. A DCM dye output coupler was used to allow better extension in the red wavelength region. Our intracavity laser photoacoustic spectrometer has been described previously.[12] The photoacoustic cell contained a Knowles Electronics EK 3132 microphone. With the addition of a small amount of water vapor to the sample, the spectra were calibrated to reference H_2O lines obtained from the HITRAN database.[13]

Theory

The oscillator strength f_{eg} of a vibrational transition from the ground state g to an excited state e is given by[14]

$$f_{eg} = 4.702 \times 10^{-7}[\text{cm D}^{-2}]\tilde{\nu}_{eg}|\mu_{eg}|^2 \qquad (1)$$

where $\tilde{\nu}_{eg}$ is the vibrational transition frequency in cm^{-1} and $\mu_{eg} = \langle e|\mu|g\rangle$ is the transition dipole moment matrix element in Debye (D). To calculate vibrational band intensities and to simulate methyl band profiles, we need to obtain both vibrational wave functions and the dipole moment function. The harmoni-

* To whom correspondence should be addressed. E-mail: henrik@alkali.otago.ac.nz. Fax: +64-3-479-7906. Phone: +64-3-479-5378.

10.1021/jp0342879 CCC: $25.00
Published on Web 05/15/2003

cally coupled anharmonic oscillator (HCAO) local mode model[8,15−17] is used to describe the methyl CH oscillators, and the methyl torsional mode is expanded in a rigid rotor basis. The details of the theoretical model that is used here are given elsewhere,[12] and we give only a brief outline. We define the methyl Hamiltonian and the methyl dipole moment function of the methyl group in a coordinate system, called the methyl coordinate system,[12] which has the *z* axis along the C−C bond around which the methyl group rotates. For molecules with two methyl groups, one methyl group is included in the model explicitly whereas the other is considered part of the frame.[12]

In the methyl coordinate system, the total Hamiltonian for a rotating CH_3 group can be approximated by

$$H_{v_1v_2v_3}/hc = \sum_{i=1}^{3}\left[\Omega F_i\left(v_i+\frac{1}{2}\right) - XF_i\left(v_i+\frac{1}{2}\right)^2\right] + VF_1 + Bm^2 - \gamma'(a_1a_2^+ + a_1^+a_2 + a_2a_3^+ + a_2^+a_3 + a_3a_1^+ + a_3^+a_1) \quad (2)$$

where $F_i = [1, \cos(\theta_i), ..., \cos(6\theta_i), \sin(\theta_i), ..., \sin(6\theta_i)]^T$, is a 13-dimensional column vector. The sixth order expansion of F_i allows the description of a V_6 potential. Both cosine and sine terms are maintained in F_i for generality, however dependent on the molecular symmetry some components might be zero.[12] θ_i is the torsional angle of the *i*th CH oscillator. Ω, X, and V are the Fourier series expansion coefficients for the frequency, anharmonicity and potential, respectively, expressed as row vectors with a dimension of 13. B is the rotational constant of the methyl group, and m is the torsional quantum number. The effective harmonic coupling constant between the methyl CH oscillators is labeled γ', and a and a^+ are the well-known harmonic oscillator ladder operators.

The dipole moment function is approximated as a series expansion in the CH stretching and torsional coordinates. We have left out the permanent dipole moment, as it does not contribute to the vibrational transition intensities. The *x* component of the dipole moment function can be written in a matrix form as

$$\mu_x = \sum_{i=1}^{3} Q_i C_x F_i \quad (3)$$

where $Q_1 = [q_1, q_1^2, q_1^3, q_1^4, q_1^5, q_1^6, q_2q_3, q_2^2q_3, q_2q_3^2]$ is a row vector and q_1, q_2, and q_3 are the displacement coordinates from the equilibrium position of the three CH bonds, respectively. The Q_2 and Q_3 vectors are obtained from Q_1 by mathematical permutation of indices in the Q_1 definition. C_x is a 9×13 matrix of dipole moment function expansion coefficients.[12] The *y* and *z* component of the dipole moment function can be obtained similarly with the expansion coefficients C_y and C_z. F_i is the Fourier series column vector as in the Hamiltonian.

The parameters and coefficients for the Hamiltonian and dipole moment function eqs 2 and 3 are obtained from a series of ab initio calculations as described in detail elsewhere.[12] In our simulation method, the observed and calculated spectra are reported in relative intensities. It has previously been found that the relative intensities within an overtone can be predicted well with the HF/6-31G(d) method.[8,17−19] We have tested the sensitivity of the simulated methyl bands to the ab initio method used for the relatively small molecules, acetic acid, acetone and acetaldehyde. We have used the Hartree−Fock (HF) and the hybrid density functional theory B3LYP, both with the 6-31G(d) and 6-311+G(d,p) basis sets. In all simulations, each vibrational transition is approximated by a Lorentzian profile with bandwidths of 20, 20, and 30 cm^{-1} for $\Delta v_{CH} = 4$, 5, and 6, respectively.

TABLE 1: Experimental and Calculated Methyl Torsional Barriers in cm^{-1}

	experimental			calculated[a]	
molecule	V_3	V_6	ref	V_3	V_6
4-methylpyridine	0	5	21	0	2
toluene	0	5	22	0	3
p-xylene	0	10	23	0	7
m-xylene	0	25	23	0	7
3-methylpyridine				53	0
2-methylpyridine	90	4	24	85	1
acetic acid	170	7	25	166	9
acetone	266		26	220	30
acetaldehyde	413	14	27	382	15
2-methylfuran	416		28	476	26
o-xylene	425	18	23	462	9

[a] With the HF/6-31G(d) ab initio method.

Results and Discussion

The series of molecules studied to understand the changes of the methyl band profile with barrier height are listed in Table 1. The experimental and HF/6-31G(d) ab initio calculated methyl torsional barriers of the molecules discussed are shown in Table 1. We have compared the methyl band profiles in the $\Delta v_{CH} = 4$ spectra of this series of molecules in Figures 1−3. These figures illustrate the evolution of the methyl band with increasing barrier height. The methyl band profiles seem to fall into one of three groups.

The methyl band profiles are nearly identical for molecules with low barriers (less than 25 cm^{-1}). The observed and simulated methyl band profiles of 4-methylpyridine (5 cm^{-1}), toluene (5 cm^{-1}), *p*-xylene (10 cm^{-1}), and *m*-xylene (25 cm^{-1}) are shown in Figure 1. In general, the methyl band profiles of molecules with quasi-free rotors are similar. In all examples, the methyl band profiles show a three peak structure.

The observed and simulated methyl band profiles of 3-methylpyridine (53 cm^{-1}), 2-methylpyridine (90 cm^{-1}), and acetic acid (170 cm^{-1}) are shown in Figure 2. The overall methyl band profile of 3-methylpyridine is similar to that of *m*- and *p*-xylene, despite it having a larger barrier and a V_3 potential instead of a V_6 potential as the low barrier examples. However, we notice a shoulder at the low energy side of the methyl band profile in 3-methylpyridine, whereas no shoulder is apparent in the corresponding methyl band profile of toluene (Figure 1). The methyl band profile of 2-methylpyridine is significantly different than the other low barrier examples. The high-energy side peak in the methyl band profile of 2-methylpyridine is diminished compared with that of 3-methylpyridine. We observe that, as the torsional barrier increases to about 100 cm^{-1}, the methyl band profile evolves in such a way that the low energy side shoulders increase in intensity. For acetic acid, the increase in barrier height to 170 cm^{-1} has clearly changed the spectrum. Compared to the simulations of the methyl profiles of the lower barrier examples, acetic acid seems less successful. However, the simulation for acetic acid does look as if the intensity is spread more, in agreement with the observed spectrum. Additional complications to the simulation of acetic acid could be the change in molecular size from the aromatic molecules to acetic acid. In our simulations, we use a Lorentzian band shape for each vibrational transition rather than taking into account the molecular rotational profiles. In a molecule like acetic acid,

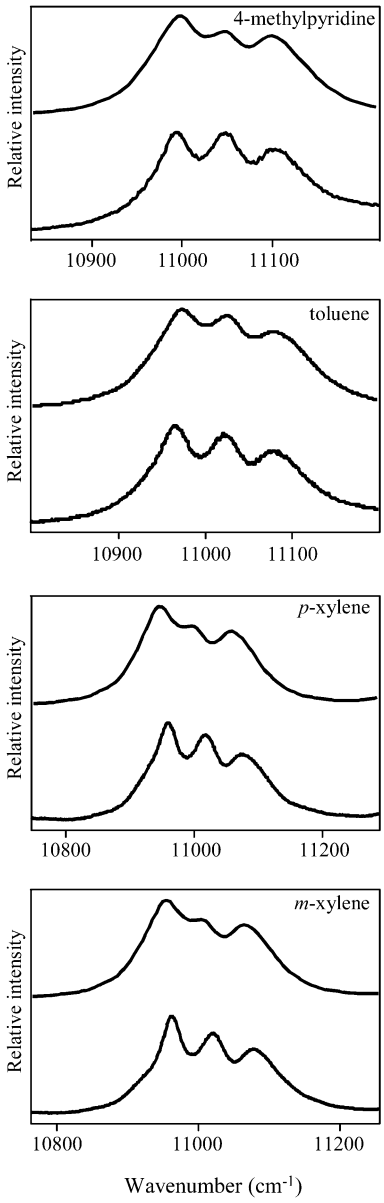

Figure 1. Observed (lower) and simulated (upper) spectra of 4-methylpyridine, toluene, *p*-xylene, and *m*-xylene in the methyl regions of $\Delta v_{CH} = 4$.

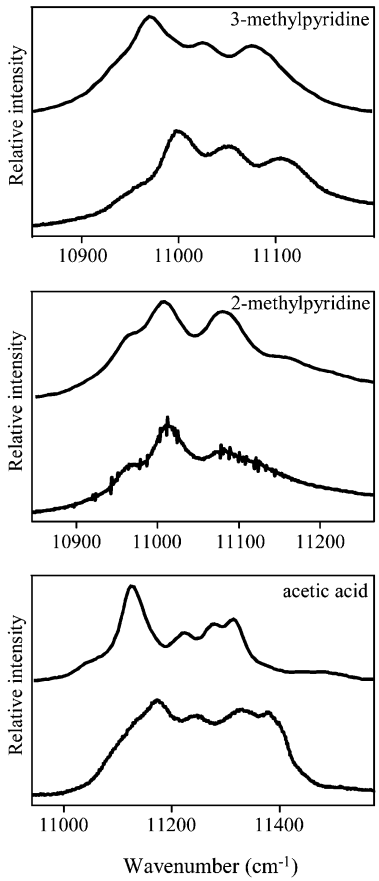

Figure 2. Observed (lower) and simulated (upper) spectra of 3-methylpyridine, 2-methylpyridine, and acetic acid in the methyl regions of $\Delta v_{CH} = 4$.

the relatively small moments of inertia would correspond to larger rotational constants that would result in a wider rotational profile.

The observed and simulated methyl band profiles of acetone (266 cm^{-1}), acetaldehyde (413 cm^{-1}), 2-methylfuran (416 cm^{-1}), and *o*-xylene (425 cm^{-1}) are shown in Figure 3. Acetone is of a similar molecular size to acetic acid, and the peaks in the band appear wider than in toluene. The methyl band profile has changed significantly relative to acetic acid. The two peak profile expected for a high barrier example starts to develop. The low energy peak seems to be split likely by a Fermi resonance. For acetaldehyde, the barrier is higher and the intensity in the central part of the spectrum has decreased compared to acetone. Perhaps the low energy shoulder in acetaldehyde is also a Fermi resonance; however, the interacting states are not as close, as indicated by the weak intensity. The methyl band profile of 2-methylfuran and *o*-xylene are similar as might be expected from their similar barrier heights. We interpret their spectra arising from a methyl group fixed in the molecular plane of the aryl ring, one peak arising from the in plane CH bond and the other peak from the two out of plane CH bonds.[8] The low energy peak is assigned to the longer out of plane CH bonds. Based on the number of bonds, we would expect the low energy peak to be more intense. In the 2-methylfuran spectrum, the central part of the methyl band profile seems slightly larger than in the *o*-xylene spectrum. This is not seen in our simulation and might suggest that the barrier in 2-methylfuran is somewhat smaller than the HF/6-31G(d) calculated value used in our calculation.

We note that in the series of molecules $R-CO-CH_3$, with R═H, CH_3, and OH, the methyl band is located at a similar frequency range for R═H and CH_3, whereas for R═OH, the methyl band has shifted to higher frequencies associated with shorter CH bond lengths.

As seen in Figures 1−3, our CH-stretching methyl torsional model simulates the methyl band profiles well for all of these molecules in the $\Delta v_{CH} = 4$ region.

In Figure 4, we compare observed and simulated methyl band profiles for acetic acid, acetone, acetaldehyde, and 2-methylfuran in the $\Delta v_{CH} = 5$ region. The simulation with our CH stretching methyl torsion model agrees with observed spectra, for these four molecules as well as for the previously studied toluene,[5] xylene,[12] and methylpyridine.[20] The Fermi resonance observed for acetone in the $\Delta v_{CH} = 4$ region seems to have disappeared in the $\Delta v_{CH} = 5$ region. For acetaldehyde, the width of the low energy portion of the $\Delta v_{CH} = 5$ band suggests Fermi resonance is occurring. The bending mode frequencies are different from molecule to molecule, and the Fermi resonance is likely to occur in different regions for different molecules.

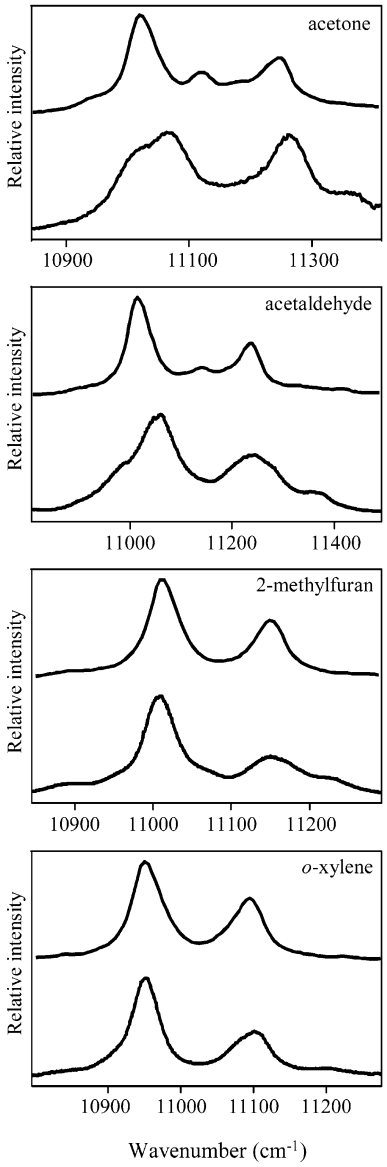

Figure 3. Observed (lower) and simulated (upper) spectra of acetone, acetaldehyde, 2-methylfuran, and *o*-xylene in the methyl regions of $\Delta v_{CH} = 4$.

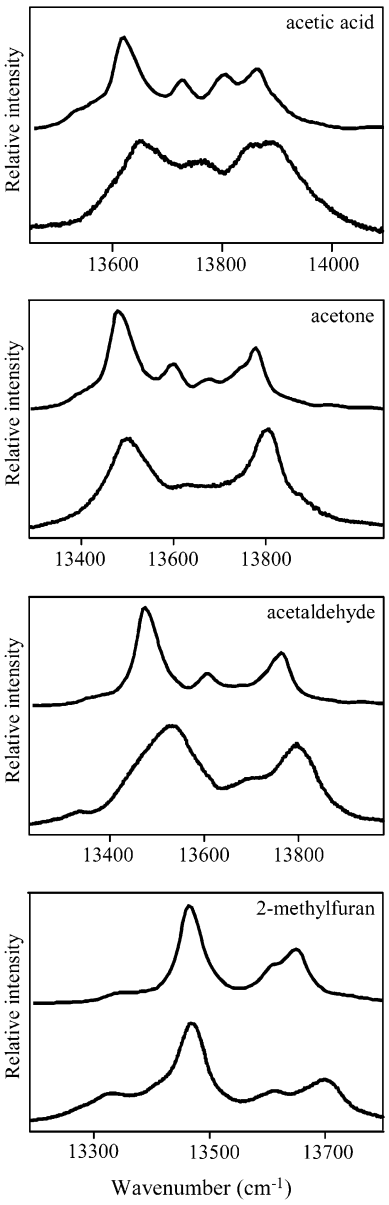

Figure 4. Observed (lower) and simulated (upper) spectra of acetic acid, acetone, acetaldehyde, and 2-methylfuran in the methyl regions of $\Delta v_{CH} = 5$.

We simulated the methyl band profiles of acetic acid, acetone, and acetaldehyde with parameters calculated with the HF/6-31G(d), HF/6-311+G(d,p), B3LYP/6-31G(d), and B3LYP/6-311+G(d,p) methods. The simulated and observed overtone spectra of acetaldehyde in the methyl $\Delta v_{CH} = 6$ region are compared in Figure 5. The simulated methyl band profiles are given in relative intensity. The spectra simulated with input parameters from the different ab initio calculations differ mainly in frequency but have similar shapes. The same outcome was found in the other overtone regions and for all three molecules. The effect of the ab initio level of theory is more significant than the basis set size. The calculated total oscillator strengths of the methyl band are given in Table 2. As can be seen in Table 2 and Figure 5, despite the band shape remaining the same, the total intensity changes between the various ab initio methods. Contrary to the methyl band profiles, the total oscillator strengths seem more dependent on the basis set size than the level of theory.

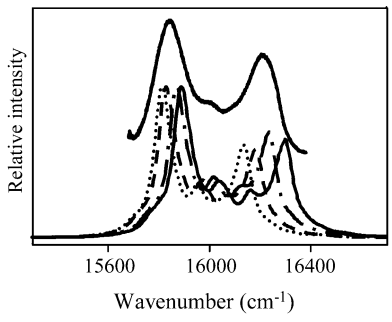

Figure 5. Observed (top) and simulated methyl overtone spectra of acetaldehyde in the regions of $\Delta v_{CH} = 6$ with the HF/6-31G(d) (···), HF/6-311+G(d,p) (- - -), B3LYP/6-31G(d) (-·-), and B3LYP/6-311+G(d,p) (—) methods.

Conclusion

We have simulated methyl band profiles in CH-stretching overtone spectra with a CH-stretching methyl torsional model. We have applied this to a series of molecules with torsional

TABLE 2: Calculated Total Methyl Oscillator Strengths of Acetaldehyde

v	HF/6-31G(d)	HF/6-311+G(d,p)	B3LYP/ 6-31G(d)	B3LYP/ 6-311+G(d,p)
1	8.4×10^{-6}	8.4×10^{-6}	5.2×10^{-6}	4.4×10^{-6}
2	1.8×10^{-7}	1.3×10^{-7}	1.8×10^{-7}	1.0×10^{-7}
3	4.0×10^{-8}	1.8×10^{-8}	4.1×10^{-8}	1.7×10^{-8}
4	5.5×10^{-9}	2.0×10^{-9}	5.0×10^{-9}	1.8×10^{-9}
5	7.9×10^{-10}	3.1×10^{-10}	6.3×10^{-10}	2.6×10^{-10}
6	1.3×10^{-10}	5.7×10^{-11}	9.5×10^{-11}	4.7×10^{-11}

barriers ranging from 5 to about 500 cm^{-1}. We have compared our simulated spectra to experimental spectra available in the literature and with our spectra of acetic acid ($\Delta v_{CH} = 4-5$) and 2-methylfuran ($\Delta v_{CH} = 4-5$). Our model has successfully explained the methyl CH-stretching overtone band structure for most barrier heights.

The methyl band profiles seem to depend more on barrier height than molecular structure. As the barrier height increases, the methyl band profiles changes from the quasi-free three peak structure to the two peak structure observed for high barrier heights. Small deviations from the quasi-free profile are seen at barrier heights around 50 cm^{-1} and are significant for barrier heights over about 100 cm^{-1}. At barrier heights of approximately 250 cm^{-1}, the methyl band profiles start to resemble that seen for high barrier heights, and above 450 cm^{-1}, little evidence of methyl rotation remains in the methyl band profile. The methyl band profile can be used as a quick guide to estimate barrier heights.

Acknowledgment. Z.R. is grateful to the University of Otago for a Specified Research Scholarship.

References and Notes

(1) Gough, K. M.; Henry, B. R. *J. Phys. Chem.* **1984**, *88*, 1298.
(2) Proos, R. J.; Henry, B. R. *J. Phys. Chem. A* **1999**, *103*, 8762.
(3) Cavagnat, D.; Lespade, L. *J. Chem. Phys.* **1997**, *106*, 7946.
(4) Zhu, C.; Kjaergaard, H. G.; Henry, B. R. *J. Chem. Phys.* **1997**, *107*, 691.
(5) Kjaergaard, H. G.; Rong, Z.; McAlees, A. J.; Howard, D. L.; Henry, B. R. *J. Phys. Chem. A* **2000**, *104*, 6398.
(6) Henry, B. R. *Acc. Chem. Res.* **1987**, *20*, 429.
(7) Durig, J. R.; Li, Y. S.; Groner, P. *J. Mol. Spectrosc.* **1976**, *62*, 159.
(8) Kjaergaard, H. G.; Henry, B. R.; Tarr, A. W. *J. Chem. Phys.* **1991**, *94*, 5844.
(9) Fang, H. L.; Meister, D. M.; Swofford, R. L. *J. Phys. Chem.* **1984**, *88*, 410.
(10) Hanazaki, I.; Baba, M.; Nagashima, U. *J. Phys. Chem.* **1985**, *89*, 5637.
(11) Kjaergaard, H. G.; Turnbull, D. M.; Henry, B. R. *J. Phys. Chem. A* **1997**, *101*, 2589.
(12) Rong, Z.; Kjaergaard, H. G. *J. Phys. Chem. A* **2002**, *106*, 6242.
(13) Rothman, L. S.; Rinsland, C. P.; Goldman, A.; Massie, S. T.; Edwards, D. P.; Flaud, J.-M.; Perrin, A.; Camy-Peyret, C.; Dana, V.; Mandin, J.-Y.; Schroeder, J.; McCann, A.; Gamache, R. R.; Wattson, R. B.; Yoshino, K.; Chance, K. V.; Jucks, K. W.; Brown, L. R.; Nemtchinov, V.; Varanasi, P. *J. Quant. Spectrosc. Radiat. Transfer* **1998**, *60*, 665.
(14) Atkins, P. W.; Friedman, R. S. *Molecular Quantum Mechanics*, 3rd ed.; Oxford University Press: Oxford, 1997.
(15) Henry, B. R. *Acc. Chem. Res.* **1977**, *10*, 207.
(16) Mortensen, O. S.; Henry, B. R.; Mohammadi, M. A. *J. Chem. Phys.* **1981**, *75*, 4800.
(17) Kjaergaard, H. G.; Yu, H.; Schattka, B. J.; Henry, B. R.; Tarr, A. W. *J. Chem. Phys.* **1990**, *93*, 6239.
(18) Kjaergaard, H. G.; Henry, B. R. *J. Chem. Phys.* **1992**, *96*, 4841.
(19) Kjaergaard, H. G.; Turnbull, D. M.; Henry, B. R. *J. Chem. Phys.* **1993**, *99*, 9438.
(20) Rong, Z.; Kjaergaard, H. G.; Henry, B. R. *J. Phys. Chem. A* **2002**, *106*, 4368.
(21) Rudolph, H. D.; Dreizler, H.; Seiler, H. *Z. Naturforsch. A* **1967**, *22*, 1738.
(22) Borst, D. R.; Pratt, D. W. *J. Chem. Phys.* **2000**, *113*, 3658.
(23) Breen, P. J.; Warren, J. A.; Bernstein, E. R.; Seeman, J. I. *J. Am. Chem. Soc.* **1987**, *109*, 3453.
(24) Dreizler, H.; Rudolph, H. D.; Maeder, H. *Z. Naturforsch. A* **1970**, *25*, 25.
(25) Demaison, J.; Dubrulle, A.; Boucher, D.; Burie, J.; Van Eijck, B. P. *J. Mol. Spectrosc.* **1982**, *94*, 211.
(26) Vacherand, J. M.; Van Eijck, B. P.; Burie, J.; Demaison, J. *J. Mol. Spectrosc.* **1986**, *118*, 355.
(27) Bauder, A.; Guenthard, H. H. *J. Mol. Spectrosc.* **1976**, *60*, 290.
(28) Norris, W. G.; Krisher, L. C. *J. Chem. Phys.* **1969**, *51*, 403.